Pergamon

Tetrahedron 55 (1999) 14599–14610

TETRAHEDRON

Conformational Analysis of Cationic (*R*,*S*)- and (*R*,*R*)-(Salen)manganese Complexes Possessing Axial Chirality as a Chiral Element Based on X-ray Crystallography: An Explanation of the Effect of Apical Ligand on Enantioselection by (Salen)manganese Catalyst

Takashi Hashihayata,[a)] T. Punniyamurthy,[a)†] Ryo Irie,[a)] Tsutomu Katsuki,[a)*]
Munetaka Akita,[b)] and Yoshihiko Moro-oka[b)]

a) Department of Molecular Chemistry, Graduate School of Science, Kyushu University 33
Higashi-ku, Fukuoka 812-8581, Japan
b) Research Laboratory of Resource Utilization, Tokyo Institute of Technology
4259 Nagatsuta, Midori-ku, Yokohama 226-8503, Japan
Received 3 September 1999; accepted 20 October 1999

Abstract: The structures of (*R*,*S*)- and (*R*,*R*)-(salen)manganese(III) complexes [(*R*,*S*)-**2a**,**b** and (*R*,*R*)-**2a**,**b**] possessing axial chirality as one of their two chiral elements were unambiguously determined by X-ray crystallographic analysis. The basal salen ligands of the complexes were demonstrated to adopt a *stepped conformation* but the degree of their non-planarity varied with the apical ligands and the relative stereochemistry of two chiral elements of the complexes. From these structural analyses, it was indicated that two factors, the chirality of the conformation of the five-membered chelate ring and the OH-π interaction between the apical aqua ligands and the 2"-phenyl group in the C3-naphthyl substituent, dictates the ligand conformation and, in turn, influences the asymmetric induction by (*R*,*S*)- and (*R*,*R*)-Mn-salen complexes.

Introduction

Catalytic asymmetric oxidation of various organic compounds is of increasing importance in synthetic chemistry. Undoubtedly, development of chiral metal catalysts has promoted the rapid progress of this area and among them chiral (salen)manganese complexes (hereafter referred to as Mn-salen complexes) are currently recognized to be the most versatile.[1] We have developed chiral Mn-salen complexes bearing four asymmetric centers at their ethylenediamine and salicylaldehyde moieties[1a,b] and achieved high enantioselectivity in various asymmetric oxidation reactions such as epoxidation, oxidation of enol ethers and sulfides, benzylic C-H oxidation, desymmetrization of *meso*-tetrahydrofurans and -pyrrolidines, and kinetic resolution of allenes, especially with the second generation Mn-salen complexes bearing a chiral binaphthyl subunit such as (*R*,*S*)- and (*R*,*R*)-**1** as catalysts.[2] Although asymmetric induction by complexes [(*R*,*S*)- and (*R*,*R*)-**1**] is influenced by the substituents on the salen ligand (R, Ar, and X), it is strongly affected by the relative configurations between the chiral binaphthyl and ethylenediamine subunits and by the presence or absence of donor ligands. The best configuration varies with the type of reaction. For example, asymmetric oxidation of sulfides and desymmetrization of *meso*-tetrahydrofurans and -pyrrolidines are well effected by

0040-4020/99/$ - see front matter
PII: S0040-4020(99)00952-7

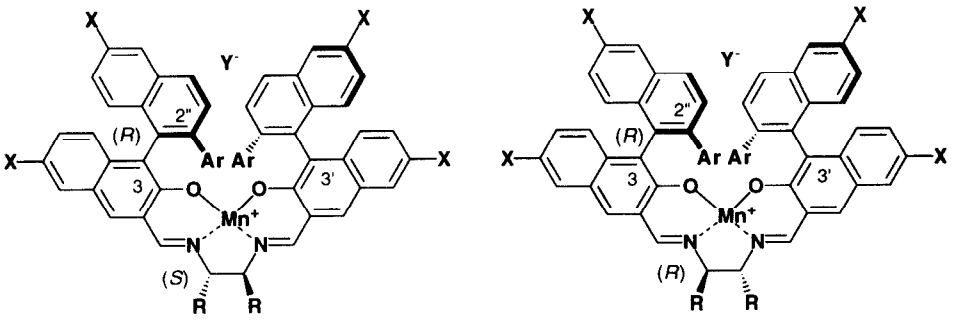

(*R*,*S*)-**1** (*R*,*R*)-**1**

Ar= C_6H_5 or *p*-[*t*-Bu(C_6H_5)$_2$Si]C_6H_4
X= H or MeO
R,R= C_6H_5, 3,5-$Me_2C_6H_3$, or -$(CH_2)_4$-
Y^-= PF_6^- or AcO^-

using (*R*,*R*)-complexes as catalysts in the absence of donor ligand, while asymmetric epoxidation, oxidation of enol ethers, and kinetic resolution of racemic allenes are better catalyzed by (*R*,*S*)-complexes in the presence of donor ligand. The issue of this substrate-specificity should be addressed by studying the structures of the active oxo Mn(V)-salen complexes but these species are too reactive to be isolated.[3] Only the presence of oxo Mn(V)-salen complexes was recently proved by MS/MS study of μ-oxo Mn(IV)-salen species,[4] still no information on their structures has been available to date. Therefore, we performed the study on the structure of Mn(III)-salen complexes[5] which have been expected to have a structure closely related to the oxo species.

The X-ray structures of several Mn(III)-salen complexes had been already determined to have slightly or shallow stepped ligand-conformation.[5a,6] On the basis of these results and in analogy with metalloporphyrin complexes, most of the mechanistic discussions had been made on the assumption that the oxo Mn(V)-salen complexes also have planar structures.[5] However, some recent results are not consistent with this assumption. For example, enantioselective epoxidation using an achiral Mn(III)-salen complex in the presence of chiral apical ligand as the catalyst[7a-c] can be explained only by assuming that the salen ligand of oxo Mn-salen species possesses high conformational freedom and takes non-planar, probably stepped conformation which had been proposed to explain the effect of C5 and C5' substituents on enantioselectivity.[8] Furthermore, the fact that Mn-salen complexes bearing a carboxylate appendage at its ethylenediamine unit shows the opposite sense of asymmetric induction to that by the usual C_2-symmetric Mn-salen complexes strongly supports our proposal that oxo Mn(V)-salen species exists in a non-planar stepped conformation (Figure 1).[7d] To clarify what factors participate in the control of the conformation of Mn-salen complexes, we studied the X-ray structures of

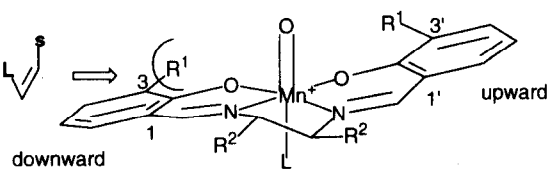

Figure 1. Proposed stepped conformation of oxo Mn(V)-salen complex and substrate approach.

complexes (*R*,*S*)-**2** and (*R*,*R*)-**2**.[9]

Results and Discussion

Cationic Mn(III)-salen complexes (*R*,*S*)-**2** and (*R*,*R*)-**2** (Figure 2) were synthesized from the corresponding acetates[10,11] by the anion exchange[12] according to the reported procedure. Recrystallization of these complexes from the appropriate solvents gave single crystals, (*R*,*S*)-**2a**, (*R*,*S*)-**2b**, (*R*,*R*)-**2a** and (*R*,*R*)-**2b** and their molecular structures were unambiguously determined by X-ray diffraction analysis as described in Figure 3. The central manganese ions of (*R*,*S*)- and (*R*,*R*)-**2a** are coordinated by two aqua ligands and those of (*R*,*S*)- and (*R*,*R*)-**2b** by cyclopentene oxide and aqua ligands at the apical sites. The selected bond lengths and angles of these complexes are shown in Table 1. The several common structural features between these complexes were observed: i) The basal salen ligands are coordinated to the manganese ion in slightly distorted square planar geometry with stepped conformation which is indicated by the deviation of the C7(7') atoms from the mean N(1)N(2)O(1)O(2) plane[13] (the side views in Figure 3). ii) The five-membered chelate rings including two imino nitrogen atoms adopt a half-chair conformation with the two phenyl substituents being disposed at pseudo-equatorial positions. iii) The phenyl substituents on the C3- and C3'-naphthalene rings are nearly perpendicular to the C3'- and C3-naphthalene rings [86° and 87° in (*R*,*S*)-**2a**, 86° and 82 ° in (*R*,*S*)-**2b**, 87° and 81° in (*R*,*R*)-**2a**, 75° and 85° in (*R*,*R*)-**2b**] and the separations between the centroids of the phenyl groups and the benzene ring units including C7' atom in the naphthalene rings [5.52 and 5.06 Å in (*R*,*S*)-**2a**, 5.14 and 4.84 Å in (*R*,*S*)-**2b**, 5.53 and 5.16 Å in (*R*,*R*)-**2a**, 5.00 and 4.89 Å in (*R*,*R*)-**2b**] are small enough for edge-to-face aromatic interaction between two aromatic groups (pointed by the double bold arrows in the views in Figure 3).[14] iv) The distances between the centroids of phenyl groups of the C3- and/or C3'-substituents and the apical oxygen atoms are very short [3.43 and 3.44 Å in (*R*,*S*)-**2a**, 3.84 Å in (*R*,*S*)-**2b**, 3.15 and 3.24 Å in (*R*,*R*)-**2a**, 3.56 Å in (*R*,*R*)-**2b**] as indicated by dotted lines, suggesting the existence of OH-π interaction between them.[15] Nonetheless, there are differences in their structures as described below.

Although complexes (*R*,*S*)-**2a** and -**2b** and (*R*,*R*)-**2a** and -**2b** differ only in the apical ligand and the chirality of the ethylenediamine unit, the sense and degree of the ligand-folding are different, respectively, as shown in Figure 3. The five membered chelate rings including manganese ion and ethylenediamine unit take a

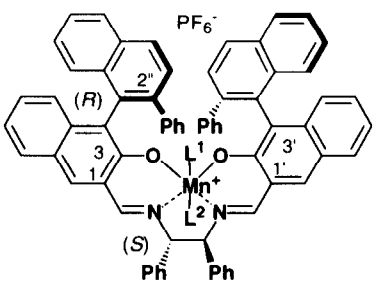

(*R*,*S*)-**2**

a: $L^1 = L^2 = H_2O$

b: L^1 = cyclopentene oxide, $L^2 = H_2O$

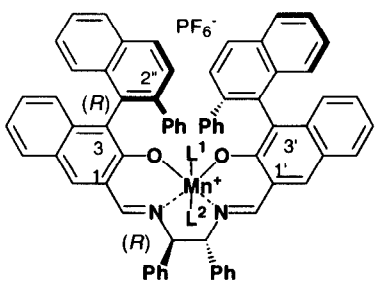

(*R*,*R*)-**2**

a: $L^1 = L^2 = H_2O$

b: L^1 = cyclopentene oxide, $L^2 = H_2O$

Figure 2.

half-chair conformation, in which manganese ion and two nitrogen atoms exist in the mean plane of the salen ligand, one methine carbon atom above the plane and the other methine carbon below the plane. Since all the substituents [manganese ion, C1 (or C1') carbon, the methine carbon next to the imino nitrogen] of the C=N double bonds roughly exist in the same plane, two C=N double bonds incline up- and down-ward, respectively, causing the ligand-folding. As the phenyl substituents at the ethylenediamine unit take a stable equatorial orientation, the sense of the folding of the chelate ring in (*R*,*S*)-**2** and (*R*,*R*)-**2** is opposite to each other. The X-

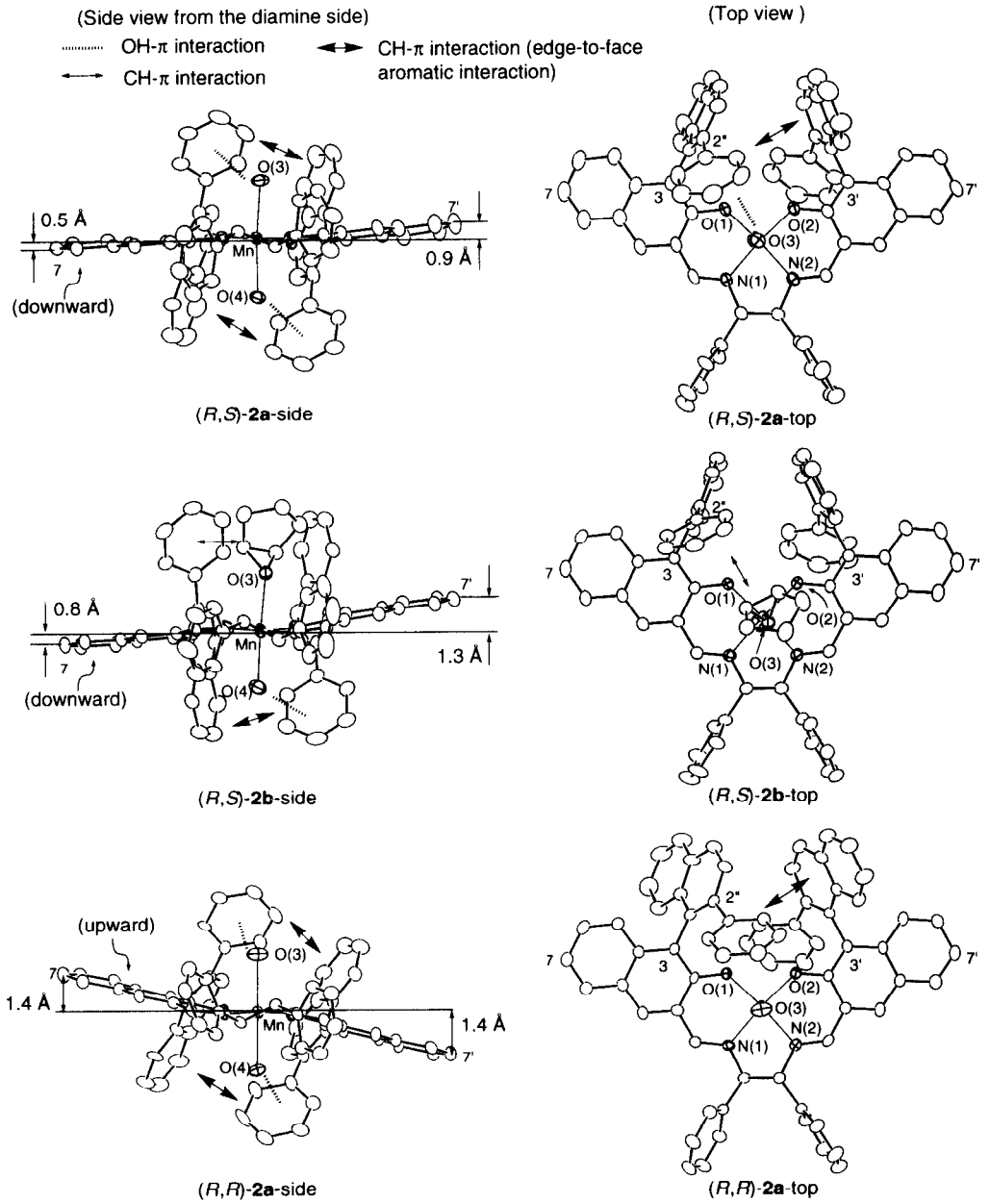

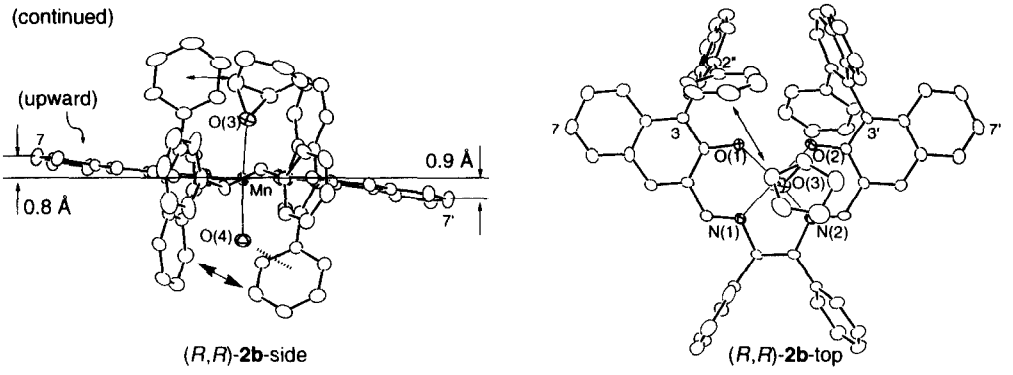

Figure 3. ORTEP diagrams of the Mn-salen cations from (*R,S*)-**2a,b** and (*R,R*)-**2a,b** with thermal ellipsoids at 30% probability level. All the hydrogen atoms have been omitted for clarity. The deviations of C7(7') atoms from the basal mean N,N,O,O-plane have been calculated by using SPARTAN on an IRIS-O2™.

ray structures of complexes (*R,S*)-**2** and (*R,R*)-**2** are consistent with this consideration. On the other hand, the degrees of the folding of the salen ligands in the four complexes are considerably different, as demonstrated by the deviation of the naphthalene rings from the mean plane of the basal salen ligands shown in Figure 3. It is noteworthy that (*R,S*)-**2a** bearing two aqua ligands at its apical positions takes a shallow stepped conformation, while (*R,R*)-**2a** bearing also two aqua ligands take a deeply folded stepped conformation. Furthermore, the replacement of one of the aqua ligand in (*R,S*)-**2a** with cyclopentene oxide increases the folding of its salen ligand, while the replacement of the aqua ligand in (*R,R*)-**2a** reduces the folding. These results indicate that, besides the chelate conformation discussed above, some other factor influences the degree of ligand-folding. As discussed above, the distances between the aqua ligand and 2"-phenyl ring are very short. This suggests that the 2"-phenyl ring and the aqua ligand attractively interact through OH-π interaction.[15] Since the OH-π interaction works similarly in (*R,S*)-**2a,b** and (*R,R*)-**2a,b**, and the effect of the chelate conformation works reverse in (*R,S*)-**2a,b** and (*R,R*)-**2a,b**, these two factors should influence synergetically in (*R,R*)-complexes and cancel out in (*R,S*)-complexes. For example, in (*R,S*)-**2a**, the OH-π interaction works to pull up the left-half of the salen ligand and down the right-half, while the chelation effect moves down the left-half of the ligand and up the right-half. Thus, two factors cancel out to each other and (*R,S*)-**2a** takes a shallow stepped conformation. On the other hand, in (*R,R*)-**2a**, two factors work synergetically to increase the ligand-folding and to shift the 2"-phenyl ring to the right side [compare the locations of the 2"-phenyl rings in (*R,S*)-**2a** and (*R,R*)-**2a**] (Figure 3).

Difference in the mutual work of two factors in (*R,S*)-**2a** and (*R,R*)-**2a** is also reflected in the distance of 2"-phenyl ring and apical aqua ligand (*vide supra*) and in the conformation of 3- and 3'-substituents. The substituents in (*R,S*)-**2a** stand almost perpendicular to the basal salen ligand, while the substituents in (*R,R*)-**2a** incline toward the apical aqua ligand.

Replacement of one of the aqua ligands with cyclopentene oxide reduces the OH-π interaction by half. Furthermore, the cyclopentane ring of the coordinated epoxide locates in the close vicinity of the 2"-phenyl ring probably due to the CH-π interaction between them [pointed by double arrows in the views of (*R,S*)-**2b** and (*R,R*)-**2b** in Figure 3].[16] Reflecting these two events, the salen ligand of (*R,S*)-**2b** folds more deeply than

Table 1. Selected bond lengths (Å) and angles (deg) for Mn-salen complexes (*R,S*)-**2a,b** and (*R,R*)-**2a,b**

	(*R,S*)-**2a**	(*R,S*)-**2b** [a]	(*R,R*)-**2a**	(*R,R*)-**2b**
Mn-O(1)	1.865(4)	1.854(3) [1.858(2)]	1.877(5)	1.870(4)
Mn-O(2)	1.847(4)	1.849(3) [1.857(3)]	1.859(5)	1.860(4)
Mn-O(3)	2.264(6)	2.342(3) [2.305(3)]	2.263(7)	2.308(5)
Mn-O(4)	2.272(5)	2.231(4) [2.224(4)]	2.286(6)	2.268(5)
Mn-N(1)	1.988(5)	1.973(4) [1.981(3)]	1.982(5)	1.987(4)
Mn-N(2)	1.970(5)	1.990(3) [1.998(3)]	2.006(6)	1.997(5)
O(1)-Mn-O(2)	92.2(2)	91.5(1) [92.7(1)]	92.1(2)	93.2(2)
O(1)-Mn-O(3)	89.6(2)	99.8(1) [96.3(1)]	91.2(2)	95.8(2)
O(1)-Mn-O(4)	92.5(2)	96.3(1) [93.5(1)]	93.3(2)	93.5(2)
O(1)-Mn-N(1)	92.5(2)	92.8(1) [92.7(1)]	93.5(2)	92.2(2)
O(1)-Mn-N(2)	174.7(2)	174.4(1) [175.2(1)]	174.9(2)	173.0(2)
O(2)-Mn-O(3)	88.4(2)	87.8(1) [88.4(1)]	95.1(2)	89.9(2)
O(2)-Mn-O(4)	87.2(2)	92.5(1) [98.0(2)]	90.2(2)	92.0(2)
O(2)-Mn-N(1)	174.2(2)	173.3(1) [171.3(1)]	173.1(2)	174.2(2)
O(2)-Mn-N(2)	93.1(2)	93.0(1) [91.9(1)]	93.0(2)	91.8(2)
O(3)-Mn-O(4)	175.2(2)	163.9(1) [168.0(1)]	172.9(2)	170.4(2)
O(3)-Mn-N(1)	95.0(2)	86.3(1) [84.3(1)]	88.8(2)	87.5(2)
O(3)-Mn-N(2)	91.2(2)	77.0(1) [82.4(1)]	88.9(2)	79.4(2)
O(4)-Mn-N(1)	89.2(2)	92.2(2) [88.5(2)]	85.4(2)	89.7(2)
O(4)-Mn-N(2)	87.1(2)	87.0(1) [87.2(1)]	86.1(2)	91.1(2)
N(1)-Mn-N(2)	82.1(2)	82.5(1) [82.6(1)]	81.4(2)	82.6(2)

a) Bond parameters in parentheses are for the other independent molecule included in an asymmetric unit. See the experimental section.

that of (*R,S*)-**2a** and the salen ligand of (*R,R*)-**2b** becomes shallower than that of (*R,R*)-**2a** [*c.f.* the side views of (*R,S*)-**2a,b**, and (*R,R*)-**2a,b**]. This attractive interaction between the C3- substituent and the apical oxide ligand may explain the ligand acceleration observed in the epoxidation of 1-alkylindene[8] and aziridination of styrene.[17]

Consideration on the Stereochemistry of Mn-Salen Catalyzed Oxidation

As discussed in the beginning of this paper, we have proposed that the salen ligands of oxo Mn(V)-salen complexes take a stepped conformation and that olefins approach from the downward benzene ring side (Figure 1).[2] That is, if the oxene atom of the oxo Mn-salen species is delivered to the top face of the complex as described in the Figure, olefins approach oxo species from its left side, orientating their bulkier olefinic substituent away from the C3-substituent of the salen ligand and give optically active epoxides.[2,18] In the epoxidation with complex (*R,S*)-**2**, the orientation of the incoming olefin is determined by the interaction between the bulkier olefinic substituent and the 2"-phenyl substituent (C3-substituent) on the ligand (Figures 1 and 3). On the other hand, in the oxidation of alkyl aryl sulfides and desymmetrization of *meso*-heterocycles which are better effected with (*R,R*)-Mn-salen complex, substrates are expected to approach the oxo species derived from (*R,R*)-Mn-salen complex from its right side and their orientation should be determined by the

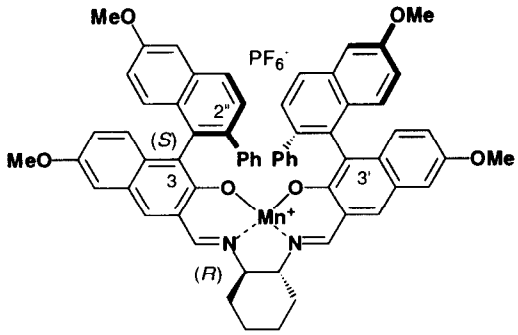

(*S*,*R*)-**3**

repulsion between the substrates and the 2"-phenyl group on C3-substituent (The 2"-substituent on C3'-substituent is located at the bottom side of the salen ligand and it can not interact with the incoming substrates). This hypothesis is compatible with the stereochemistry observed in oxidation of sulfides with (*S*,*R*)-Mn-salen complex **3**[19] as a catalyst.[20] As a matter of course, these results strongly suggest that the 2"-phenyl group on C3-substituent in (*R*,*R*)-Mn-salen complex should be located close to the path of the incoming substrate from the right and the 2"-phenyl group on C3-substituent in (*R*,*S*)-Mn-salen complex to the path from the left, in the corresponding oxo Mn-salen species.

As discussed above, Mn-salen complexes take stepped conformation. Oxo Mn-salen complexes are considered to adopt more deeply folded stepped conformation, since the length of the Mn-$O_{equatorial}$ bond is expected to shorten and the non-planarity of its basal salen ligand is amplified as the oxidation state of the manganese ion becomes higher.[21] Therefore, the factors controlling the conformation of the ligand of Mn-salen ligand are considered to hold for the control of the ligand-conformation of the corresponding oxo Mn-salen complex. Thus, clarification of the conformation-controlling factors enabled us to answer the above question about the location of 2"-phenyl group in (*R*,*S*)- and (*R*,*R*)-complexes and another question why oxidations with (*R*,*S*)-complexes are efficiently performed in the presence of a donor ligand but oxidations with (*R*,*R*)-complexes in the absence of a donor ligand. As discussed above, degree of the folding of salen ligand and the conformation of its C3-substituent is dictated by three factors: i) conformation of the five-membered chelate ring, ii) the OH-π interaction between the apical aqua ligand and 2"-phenyl group and iii) the edge-to-face aromatic interaction between C3- and C3'-substituents. As discussed above, the substrate is considered to approach oxo species from the side of the downward naphthalene ring. However, (*R*,*S*)-**2a** adopts a shallow stepped conformation. Therefore, upon the oxidation of (*R*,*S*)-**2a** to the corresponding oxo species, its ligand-folding is desired to be deepened and its 2"-phenyl group to shift close to the substrate-approaching path from the left side. On the other hand, (*R*,*R*)-**2** that is already deeply folded disposing the 2"-phenyl group close to the apical ligand is desired to be oxidized to the corresponding oxo species, maintaining its conformation and the location of the 2"-phenyl group. The desired conformational change in the oxidation of (*R*,*S*)-**2a** to the oxo species should be achieved by adding a donor ligand such as 4-phenylpyridine *N*-oxide which replaces the remaining apical aqua ligand and eliminates the unnecessary OH-π interaction that conflicts with the effect of the five-membered chelate ring and forces (*R*,*S*)-**2a** to adopt a shallow stepped conformation. This prediction is supported by the difference in the conformation of (*R*,*S*)-**2a** and (*R*,*S*)-**2b** in which one of the aqua ligand is

replaced by epoxy ligand: i) Ligand-folding in (*R*,*S*)-**2b** is larger than that of (*R*,*S*)-**2a** and the 2"-phenyl group in the former is located closer to the approaching path from the left side than the 2"-phenyl group in the latter (Figure 3). On the other hand, replacement of the aqua ligand in the oxo species derived from (*R*,*R*)-**2a** eliminates the necessary OH-π interaction that draws 2"-phenyl group toward the right side. Again, this prediction is supported by comparison of the conformation of (*R*,*R*)-**2b** and (*R*,*R*)-**2a**. Coordination of epoxy ligand as an apical ligand reduces the ligand-folding and shifts the 2"-phenyl group to the undesired left side. These considerations agree with the fact that oxidations with (*R*,*S*)-Mn-salen complexes should be carried out in the presence of donor ligand and oxidations with (*R*,*R*)-complexes in the absence of donor ligand.[2]

Conclusion

We were able to determine the structures of (*R*,*S*)- and (*R*,*R*)-Mn-salen complexes [(*R*,*S*)-**2a,b** and (*R*,*R*)-**2a,b**] by X-ray crystallographic analyses. The central manganese ions in these complexes take octahedral geometry and the salen ligands coordinate manganese ions in square planar geometry. All the salen ligands adopt stepped conformation due to the half-chair conformation of the five-membered chelate rings including manganese ion and the ethylenediamine unit. Since the five-membered chelate ring adopts the half-chair conformation in which the substituents at the ethylenediamine are delivered in equatorial position, (*R*,*S*)- and (*R*,*R*)-Mn-salen complexes fold in an opposite way. On the other hand, analyses of the structures of complexes and their comparison indicate the presence of OH-π attractive interaction between aqua ligand and 2"-phenyl group. Combination of these two effects enables for second generation Mn-salen complexes to adopt various types of ligand-conformation. (*R*,*S*)-Complex **2a** takes a shallow stepped conformation, as the effects of the five-membered chelate ring and OH-π interaction on ligand-folding cancel out, while (*R*,*R*)-complex **2a** adopts a deep stepped conformation as two effects work synergetically there. This endows second-generation Mn-salen complexes with versatile catalytic activity.[2] Contrast to this, the conformation of first-generation Mn-salen complexes bearing bulky groups such as *t*-butyl group at C3 and C3'-carbons is dictated only by the conformation of the five-membered chelate ring. Finally, we were able to disclose that the ligand conformation of Mn-salen complexes is strongly related to their asymmetric catalysis and its appropriate control expands the scope of Mn-salen catalyzed asymmetric reactions. The finding on the role of the apical aqua ligand in chiral cationic Mn-salen catalysts may also give a rational for understanding the catalysis of cationic complexes bearing aqua ligand(s).[22] Recently several examples that the addition of water to asymmetric reaction systems affects their enantioselectivity have been reported[23] but the role of water molecule was not sufficiently evaluated. The present study will also shed some light on this area of chemistry.

Experimental Section

Details for X-ray crystallographic analyses: Cationic Mn-salen complexes (*R*,*S*)-**2** and (*R*,*R*)-**2** were synthesized by treatment of the corresponding acetate[10,11] with sodium hexafluorophosphate and purified by silica gel column chromatography (CH_2Cl_2-MeOH= 9:1) according to the reported procedures.[12] Four single crystals of (*R*,*S*)-**2a,b** and (*R*,*R*)-**2a,b** were obtained by recrystallization from $CHCl_3$-toluene, cyclopentene oxide-toluene-heptane, CH_2Cl_2-hexane, and cyclopentene oxide-toluene-heptane under air, respectively. The samples of (*R*,*S*)-**2a,b** and (*R*,*R*)-**2a** were immersed in hexane and transported from Kyushu University to

Tokyo Institute of Technology. Anal. Calcd for $C_{75}H_{65}N_2O_4F_6PCl_3Mn$ [(*R*,*S*)-**2a**·$CHCl_3$·hexane]: 66.01; H, 4.80; N, 2.05. Found: C, 66.15; H, 4.34; N, 2.11. Calcd for $C_{76.5}H_{60}N_2O_4F_6PMn$ [(*R*,*S*)-**2b**·(toluene)$_{1/2}$]: C, 72.28; H, 4.76; N, 2.20. Found: C, 72.55; H, 4.82; N, 2.19. Calcd for $_{68}H_{50}N_2O_4F_6PMn$ [(*R*,*R*)-**2a**]: C, 70.45; H, 4.35; N, 2.42. Found: C, 70.21; H, 4.41; N, 2.38. Calcd for $C_{73}H_{60}N_2O_6F_6PMn$ [(*R*,*R*)-**2b**·$2H_2O$]: C, 69.52; H, 4.80; N, 2.22 Found: C, 69.35; H, 5.14 N, 2.01. Suitable crystals were mounted on glass fibers and diffraction measurements were made on a Rigaku RAXIS IV [(*R*,*S*)-**2a**,**b** and (*R*,*R*)-**2a**] or a Rigaku RAXIS RAPID [(*R*,*R*)-**2b**] imaging plate area detector with Mo Kα radiation (λ= 0.71069 Å). The data collections were carried out at -60 °C [(*R*,*S*)-**2a**,**b** and (*R*,*R*)-**2a**] or at -90 °C [(*R*,*R*)-**2b**]. Indexing was performed from 3 oscillation images which were exposed for 4 min [(*R*,*S*)-**2a**,**b** and (*R*,*R*)-**2a**] or from 2 oscillation images which were exposed for 5 min [(*R*,*R*)-**2b**]. The crystal-to-detector distance was 100 mm [(*R*,*S*)-**2a**,**b** and (*R*,*R*)-**2a**] and 124 mm [(*R*,*R*)-**2b**]. Data collection parameters were as follows: the detector swing angle: 3° [(*R*,*S*)-**2a**], 3.5° [(*R*,*S*)-**2b**], 2.5° [(*R*,*R*)-**2a**], 5° [(*R*,*R*)-**2b**]; the number of oscillation images: 25 [(*R*,*S*)-**2a**], 51 [(*R*,*S*)-**2b**], 50 [(*R*,*R*)-**2a**], 44 [(*R*,*R*)-**2b**]; the exposed time: 100 min [(*R*,*S*)-**2a**], 27 min [(*R*,*S*)-**2b**], 50 min [(*R*,*R*)-**2a**], 25 min [(*R*,*R*)-**2b**]. Readout was performed with the pixel size of 100 μm x 100 μm. The structural analysis was performed on an IRIS O2 computer using teXsan structure solving program system obtained from the Rigaku Corp., Tokyo, Japan. Neutral scattering factors were obtained from the standard source.[24] In the reduction of data, Lorentz and polarization corrections were made. An empirical absorption correction[25] or a symmetry-related absorption correction using ABSCOR (a program obtained from the Rigaku Corp., Tokyo, Japan) was also applied for (*R*,*S*)-**2a**,**b** and (*R*,*R*)-**2a** or (*R*,*R*)-**2b**, respectively. The structures were solved by the direct methods (SHELXS-86) and refined (on F^2) using SHELXL-93 linked to teXsan.

Details of the refinements are as follows. Mn(III)-salen (*R*,*S*)-**2a**: All the non-hydrogen atoms were refined anisotropically. All the hydrogen atoms except for the H_2O hydrogen atoms were fixed at the calculated positions (C-H: 0.95 Å) and not refined, and the H_2O hydrogen atoms were refined isotropically. Mn(III)-salen (*R*,*S*)-**2b**: Two independent molecules with essentially the same geometry of the cationic parts are included in an asymmetric unit. All the non-hydrogen atoms were refined anisotropically. The hydrogen atoms of the aqua ligand were located by Fourier synthesis and all the hydrogen atoms of the cationic part were fixed at the calculated positions (C-H: 0.95 Å) and not refined. The hydrogen atoms of the water molecules (O11-O14) and the methyl hydrogen atoms of the toluene solvates were not included in the refinement. The occupancy factor of O14 was refined to be 0.66. During the course of the refinement it was found that PF_6 anion was disordered. The axial F atoms (F1b and F2b), however, could not be resolved and only equatorial F atoms were refined by taking into account two contributors (F3b-6b : F3c-6c= 1 : 1). Mn(III)-salen (*R*,*R*)-**2a**: All the non-hydrogen atoms were refined anisotropically. During the refinement, it was found that the F_6 parts in the PF_6 anion was disordered and two components were considered (F1-6 : F1a-6a= 0.6 : 0.4). The hydrogen atoms except those of the aqua ligands (not located) were located at the calculated positions and not refined. Although this severe disorder of PF_6^- renders the *R* value slightly higher, the small values of all the temperature factors of the atoms of the cationic part allow us to discuss the detailed structure of the cationic part.[25] Mn(III)-salen (*R*,*R*)-**2a** and (R,R)-**2b**: All the non-hydrogen atoms were refined anisotropically. The hydrogen atoms except those of the aqua ligand (not located) were located at the calculated positions (C-H: 0.95 Å) and not refined. The hydrogen atoms of the aqua ligand were not included in the refinement.

Crystallographic Data for these Mn-salen complexes are summarized in Tables 2 and 3. [26]

Table 2. Crystallographic Data for Mn-salen complexes (*R,S*)-**2a**·$(H_2O)_{1.92}$·$(toluene)_{1/2}$ and (*R,S*)-**2b**·$CHCl_3$·hexane

	(*R,S*)-**2a**·$CHCl_3$·hexane	(*R,S*)-**2b**·$(H_2O)_{1.92}$·$(toluene)_{1/2}$
empirical formula	$C_{75}H_{65}N_2O_4F_6PCl_3Mn$	$C_{76.5}H_{64.16}N_2O_{5.83}F_6PMn$
formula weight	1364.6	1305.8
crystal system	monoclinic	monoclinic
space group	$P2_1$	$C2$
a / Å	11.053(2)	44.630(6)
b / Å	19.163(4)	11.070(1)
c / Å	15.90(1)	26.482(6)
β / deg	95.84(3)	103.074(5)
V / Å^3	3350(1)	12744(4)
Z	2	8
D_{calcd} / g cm^{-3}	1.35	1.36
μ(Mo-Kα) / cm^{-1}	4.08	3.07
maximum 2θ / deg	55.1	55.1
no of data collected	6656	14516
no of unique data	6161 [$I > 2.0\sigma(I)$]	13780 [$I > 2.0\sigma(I)$]
no of parameters refined	845	1705
reflection/parameter ratio	7.29	8.08
$R1$,wR_2[c]	0.084, 0.212	0.064, 0.170
goodness of fit	1.70	1.24

Table 3. Crystallographic Data for Mn-salen complexes (*R,R*)-**2a** and (*R,R*)-**2b**

	(*R,R*)-**2a**	(*R,R*)-**2b**
empirical formula	$C_{68}H_{50}N_2O_4F_6PMn$	$C_{73}H_{56}N_2O_4F_6PMn$
formula weight	1159.06	1225.17
crystal system	orthorhombic	monoclinic
space group	$P2_12_12_1$	$P2_1$
a / Å	19.713(2)	11.4490(5)
b / Å	10.9097(9)	11.3890(5)
c / Å	26.597(2)	22.780(1)
β / deg		91.399(1)
V / Å^3	5719.9(8)	2969.4(2)
Z	4	2
D_{calcd} / g cm^{-3}	1.346	1.370
μ(Mo-Kα) / cm^{-1}	3.30	3.22
maximum 2θ / deg	55.1	55.0
no of data collected	6497	6742
no of unique data	6123 [$I > 2.0\sigma(I)$]	4591 [I> 2.0$\sigma(I)$]
no of parameters refined	793	784
reflection/parameter ratio	7.72	6.92
$R1$,wR_2[c]	0.091, 0.234	0.056, 0.165
goodness of fit	1.52	0.98

Acknowledgment

The authors are grateful to Prof. Tomoji Ozeki at Tokyo Institute of Technology for his technical assistance in crystal structure analysis. Financial support from Grant-in-Aid for Scientific Research on Priority Areas, No. 706: Dynamic Control of Stereochemistry (to T.K.) and Grant-in-Aid for Specially Promoted Research No. 08102006 (to Y.M.) from the Ministry of Education, Science, and Culture, Japan, is gratefully acknowledged.

References and Notes

† Postdoctoral Research Fellow of the Japan Society for the Promotion of Science.

1. a) Katsuki, T. *Coord. Chem. Rev.* **1995**, *140*, 189. b) Katsuki, T. *J. Synth. Org. Chem. Jpn.* **1995**, *53*, 940. c) Jacobsen, E. N. In "Catalytic Asymmetric Synthesis" ed by I. Ojima, VCH publishers, Inc., New York, (1993), pp 159. d) Jacobsen, E. N. In "Comprehensive Organometallics Chemistry II"; Wilkinson, G., Stone, F. G. A., Abel, E. W., and Hegedus, L. S. I., eds.; Vol.12, Pergamon Press, New York (1995).
2. Ito, Y. N.; Katsuki, T. *Bull. Chem. Soc. Jpn.*, **1999** , *72*, 603.
3. Srinivasan, K.; Michaud, P.; Kochi, J. K. *J. Am. Chem. Soc.*, **1986** , *108*, 2309.
4. Feichtinger, D.; Plattner, D. A. *Angew. Chem. Int. Ed. Engl.*, **1997** , *36*, 1718.
5. (a) Zhang, W.; Loebach, J. L.; Wilson, S. R.; Jacobsen, E. N. *J. Am. Chem. Soc.*, **1990**, *112*, 2801. (b) Jacobsen, E. N.; Zhang, W.; Muci, L. C.; Ecker, J. R.; Deng, L. *J. Am. Chem. Soc.*, **1991**, *113*, 7063. (c) Irie, R.; Noda, K.; Ito, Y.; Matsumoto, N.; Katsuki, T. *Tetrahedron: Asymmetry*, **1991**, *2*, 481. (d) Hosoya, N.; Hatayama, A.; Yanai, K.; Fujii, H.; Irie, R.; Katsuki, T. *Synlett*, **1993**, 641.
6. (a) Rispens, M. T.; Meetsma, A.; Feringa, B. L. *Recl. Trav. Chim. Pays-Bas.*, **1994**, 113, 413. (b) Pospisil, P. J.; Carsten, D. H.; Jacobsen, E. N. *Chem. Eur. J.*, **1996**, *2* 974. (c) Finney, N. S.; Pospisil, P. J.; Chan, S.; Palucki, M.; Konsler, R. G.; Hansen, K B.; Jacobsen, E. N. *Angew. Chem. Int. Ed. Engl.*, **1997** , *36*, 1720. See also note 5a.
7. a) Hashihayata, T.; Ito, Y. N.; Katsuki, T. *Synlett* **1996**, 1079. b) *Idem*, *Tetrahedron*, **1997**, *53*, 9541. c) Miura, K.; Katsuki, T. *Synlett* **1999** , 783. d) Ito, Y. N.; Katsuki, T. *Tetrahedron Lett.*, **1998** , *39*, 4325.
8. Noguchi, . N.; Irie, R.; Fukuda, T.; Katsuki, T. *Tetrahedron Lett.* **1996** , *37*, 4533.
9. For the preliminary accounts of this study, see: a) Irie, R.; Hashihayata, T.; Katsuki, T.; Akita, M.; Moro-oka, Y. *Chem. Lett.*, **1998**, 1041. b) Punniyamurthy, T.; Irie, R.; Katsuki, T; Akita, M.; Moro-oka, Y. *Synlett* **1999** , 1049.
10. Hosoya, N.; Hatayama, A.; Irie, R.; Sasaki, H.; Katsuki, T. *Tetrahedron* **1994** , *50*, 4311.
11. a) Punniyamurthy, T.; Miyafuji, A.; Katsuki, T. *Tetrahedron Lett.* **1998**, *39*, 8295. b) Punniyamurthy, T.; Katsuki, T.; *Tetrahedron* **1999** , *55*, 9439.
12. Irie, R. Ph.D. thesis, Kyushu University; December 1995.
13. The mean equatorial planes [N(1)-N(2)-O(2)-O(1)] of (*R,S*)- and (*R,R*)-complexes **2a** and **2b** are slightly distorted as indicated by deviations of each atom from the planes: In the order of N(1), N(2), O(2), O(1) atoms, -0.02, +0.02, -0.02, +0.02 Å for (*R,S*)-**2a**, +0.05, -0.05, -0.05, +0.05 Å for (*R,S*)-**2b**, -0.03, +0.03, -0.03, +0.03 Å for (*R,R*)-**2a**, and -0.03, +0.03, -0.03, +0.03 Å for (*R,R*)-**2b** (the plus and minus signs indicate that the atom is positioned above and below the planes, respectively). The plane was so defined as to minimize the sum of square of the deviations of each atom from the plane. All the calculations were done by using SPARTAN on an IRIS-O2™.
14. The dihedral angles of and the separations between the centroids of the interacting aromatic pairs fall in the range of 30-90° and 4.5-7 Å. Burley, S. K.; Petsko, G. A. *Science* **1985** , *229*, 23.
15. Suzuki, S.; Green, P. G.; Bumgarner, R. E.; Dasgupta, S.; Goddard III, W. A.; Blake, G. A. *Science*, **1992** , *257*, 942.
16. Nishikori, H.; Katsuki, T. *Tetrahedron Lett.* **1996** , *37*, 9245.
17. The closest contacts between the hydrogen atoms which are generated at the α carbon atoms of the apical

epoxides from ideal geometry with C-H 1.10 Å and the carbon atoms of 2"-phenyl groups [respectively, 2.87 Å for (*R,S*)-**2b** and 2.91Å for (*R,R*)-**2b**] are shorter than the sum of van der Waals radii of hydrogen and carbon atoms. Nishio, M.; Hirota, M. *Tetrahedron*, **1989**, *45*, 7201. Jorgensen, W. L.; Severance, D. L. *J. Am. Chem. Soc.*, **1990** , *112*, 4768.

18. The following discussions in this paper are all based on the assumption that the metal-oxo bond is formed at the top face of the complexes. However, since the parent Mn-salen complexes are C2-symmetric, the oxo species having the oxene atom at bottom face are the same ones as the oxo species at top face.
19. Due to the *R,S*-nomenclature system, the configuration of the methoxylated binaphthyl unit in **3** is designated to be *S* but it is the same as the configuration (*R*) of the non-methoxylated binaphthyl unit in (*R,R*)-**2**.
20. a) Noda, K.; Hosoya, N.; Irie, R.; Yamashita, Y.; Katsuki, T. *Tetrahedron*, **1994**, *50*, 9609. b) Kokubo, C.; Katsuki, T. *Tetrahedron*, **1996** , *52*, 13895.
21. A similar trend has been observed in comparison between a series of Cr-salen complexes, cationic oxo Cr(V)-salen complex, its pyridine *N*-oxide adduct (reference 27) and Cr(III)-salen azide complex (reference 28), the structures of which have been determined unambiguously by X-ray diffraction study. The basal ligands of all these three Cr-salen complexes take stepped conformation, but the Cr-$O_{equatorial}$ bond length gets longer and the degree of the ligand-folding reduces in this order: The Cr-$O_{equatorial}$ bond lengths are *ca.* 1.81Å for cationic Cr(V), *ca.* 1.84Å for Cr(V)-pyridine *N*-oxide adduct (reference 27), and *ca.* 1.90-1.92Å for Cr(III)-salen azide complex (reference 28).
22. For asymmetric catalyses of chiral cationic complexes bearing aqua ligands, see: a) Odenkirk, W.; Bosnich, B. *J. Chem. Soc., Chem. Commun.*, **1995**, 1181. b) Desimoni, G.; Faita, G.; Righetti, P. R. *Tetrahedron Lett.*, **1996**, *37*, 3027. c) Desimoni, G.; Faita, G.; Invernizzi, G. A.; Righetti, P. R. *Tetrahedron*, **1997**, *53*, 7671. d) Gothelf, K. V.; Hazell, R. G.; Jørgensen, K. R. *J. Org. Chem.*, **1998**, *63*, 5483. e) Sodeoka, M., Tokunou, R.; Miyazaki, F.; Hagiwara, E.; Shibasaki, M. *Synlett*, **1997**, 463. f) Kanemasa, S.; Oderatoshi, Y.; Yamamoto, H.; Tanaka, J.; Wada, E.; Curran, D. P. *J. Org. Chem.*, **1997**, *62*, 6454. g) Kanemasa, S.; Oderatoshi, Y.; Sakaguchi, S.-I.; Yamamoto, H.; Tanaka, J.; Wada, E.; Curran, D. P. *J. Am. Chem.* Soc., **1998**, *120*, 3074. h) Kanemasa, S.; Oderatoshi, Y.; Tanaka, J.; Wada, E. *J. Am. Chem.* Soc., **1998**, *120*, 12355. i) Ghosh, A. K.; Cho, H.; Cappiello, J. *Tetrahedron: Asymmetry*, **1998** , *9*, 3687.
23. a) Sasai, H.; Suzuki, T.; Arai, S.; Arai, T.; Shibasaki, M.; *J. Am. Chem. Soc.*, **1992**, *114*, 4418. b) Sasai, H.; Suzuki, T.; Itoh, N.; Shibasaki, M.; *Tetrahedron Lett.*, **1993**, *34*, 851. c) Mikami, K.; Kotera, O.; Motoyama, Y.; Sakaguchi, H. *Synlett*, **1995**, 975. d) Watanabe, S; Kobayashi, Y.; Arai, T.; Sasai, H.; Bougauchi, M.; Shibasaki, M. *Tetrahedron Lett.*, **1998**, *39*, 7353. e) Fujimura, O. *J. Am. Chem.* Soc., **1998** , *120*, 10032. See also the references 14.
24. Cromer, D. T.; Waber, J. T. "*International Tables for X-ray Crystallography*", Kynoch Press: Birmingham, England, 1975; Vol. 4.
25. Stuart, D; Walker, N. *Acta Cryst.* **1979** *A35*, 925.
26. Details of the X-ray crystallographic data for the Mn-salen complexes reported herein are available on request from the Cambridge Crystallographic Data Center, 12 Union Road, Cambridge, CB2 1EZ, U.K.
27. Srinivasan K., Kochi, J. K. *Inorg. Chem.*, **1985** , *24*, 4671.
28. Hansen, K. B.; Leighton, J. L.; Jacobsen, E. N.; *J. Am. Chem.* Soc., **1996** , *118*, 10924.